Research Article

Journal of PeptideScience

Received: 30 March 2010 Revised: 12 May 2010 Accepted: 12 May 2010 Published online in Wiley Interscience: 13 July 2010

(www.interscience.com) DOI 10.1002/psc.1260

Determination of an unusual secondary structural element in the immunostimulating tetrapeptide rigin in aqueous environments: insights via MD simulations, ^{1}H NMR and CD spectroscopic studies

Nigam Kumar and Raghuvansh Kishore*

An immunomodulating tetrapeptide, rigin (H-Gly-Gln-Pro-Arg-OH), has been examined for its secondary structure preferences through combined use of high-temperature unrestrained MD simulations in *implicit* water and 1D and 2D ^{1}H NMR spectroscopy. The distribution of backbone torsion angles revealed the predominance of *trans* conformers across the Xaa-Pro peptide bond. The results of MD simulations revealed that of the five predicted families A–E, the predominant families, family A (92 structures), family C (63 structures) and family D (31 structures), could be complemented by extensive 1D and 2D ^{1}H NMR parameters acquired in aqueous PBS solution. A survey of specific inter- and intraresidue NOEs substantiated the predominance of an unusual type VII β-turn structure, defined by two torsion angles, i.e. $\psi_{Gln} \sim 155^\circ$ and $\phi_{Pro} \sim -65^\circ$ across the Gln-Pro segment. The proposed semi-folded *kinked* topology precluded formation of any intramolecular interaction, i.e. hydrogen bond or electrostatic interaction. Far-UV CD spectral characteristics of rigin in aqueous PBS solution and non-aqueous structure-promoting organic solvents, TFE and TMP, revealed its strong solvent dependence. However, in aqueous PBS solution, the presence of a weak negative shoulder at ~ 234 nm could be ascribed to a small population with ordered, semi-folded topology. We propose that the plausible structural attributes may be exploited for design and rigidification of the bioactive conformation of this immunomodulator toward improved immunopharmacological properties.

Supporting information may be found in the online version of this article

Keywords: bioactive peptide; conformational analysis; unusual *kinked* topology; MD simulations; *implicit* water; spectroscopic studies

Introduction

Rigin, an immunostimulating tetrapeptide (Gly^{341}-Gln-Pro-Arg^{344}) that connects the C_H2 and C_H3 domains of human IgG molecule, has been shown to exhibit significant *in vitro* phagocytosis-stimulating activity toward rat blood leukocytes and *Staphylococcus aureus* [1–4]. The reported phagocytosis index of rigin [1,2] has been found to be same as that of another structurally related immunostimulating tetrapeptide, tuftsin (Thr^{289}-Lys-Pro-Arg^{292}), located in the C_H2 domain, which has been extensively investigated for its structure–function relationship [3,5–9]. Rigin is capable of efficiently releasing interleukin-1 and α-tumor necrosis factor from human monocytes and displacing [^{3}H]-tuftsin from macrophages at significantly high concentrations of $\sim 10^{-4}$ M [2]. To develop potent rigin derivatives capable of exhibiting enhanced phagocytosis activity, Rocchi *et al*. [2] initially attempted the chemical synthesis and bioactivity evaluation of a few glycosylated derivatives; however, these failed to augment the phagocytosis-stimulating activity.

The presumption that endogenous peptide immunomodulators generate physiological responses in target cells via their specific surface receptor suggests that rigin may activate macrophage binding to its own specific receptor, i.e. other than tuftsin receptor [2]. The two immunomodulators may be considered similar but not identical and such closely related peptide sequences provide excellent biological probes to elucidate biological processes for understanding their specific functions in living systems. Despite undoubted therapeutic potential utility of these immunomodulators, only limited reports exists in respect of rigin's structure–function relationships [2,4,10–12]. Although the chemical identity of rigin has been described more than three decades ago, unlike with tuftsin [13,14], no attempt has been

* *Correspondence to: Raghuvansh Kishore, Protein Science & Engineering Division, Institute of Microbial Technology, Sector 39-A, Chandigarh - 160 036, India. E-mail: kishore@imtech.res.in*

Protein Science & Engineering Division, Institute of Microbial Technology, Sector 39-A, Chandigarh - 160 036, India

Abbreviations used: *1D, one-dimensional; 2D, two-dimensional; MPLC, medium performance liquid chromatography; PBS, phosphate-buffered saline; RMSD, root mean square deviations; TFA, trifluoroacetic acid; TMP, trimethylphosphate; TNCG, truncated Newton conjugated gradient; WATERGATE, WATER suppression GrAdient Tailored Excitation.*

Journal of PeptideScience

made to identify and characterize the rigin receptor. The lack of any structural information about rigin's receptor precludes rational design approaches and therefore characterization of preferred molecular conformations in solution might be valuable for initiating structure-based design of this immunopharmacophore.

The investigation of conformational characteristics of bioactive peptides in different environments is key to understand the nature of 'conformational collections' that predominate in solution conditions. Theoretical approaches such as MD simulations have been supportive in exploring the energetically preferred conformational space that may be accessible to short peptides [15–17]. One of the principal goals of our investigation is to execute systematic MD simulations of rigin in *implicit* solvents and compare its conformational characteristics acquired under different environmental conditions. Previously, using high-temperature quenched MD simulations under the influence of distance-dependent dielectric ($\varepsilon = r_{ij}$), we elucidated the conformational preferences of rigin as a tightly folded *distorted* type III β-turn structure stabilized by a salt bridge, i.e. Gly $H_3N^+ \cdots COO^-$ Arg interaction [12]. Also, we established a synergy between the high-temperature MD simulations in *implicit* DMSO and 1D and 2D ^{1}H NMR-derived parameters acquired in DMSO-d_6 solution [10,11]. It may be emphasized that MD simulations with *implicit* solvent models have become an established tool to analyze biomolecular structures and dynamics, complementary to experimental techniques, and gained widespread acceptance [18–20].

Our interest in this immunomodulator arose from the research aimed at exploring systematically the most probable molecular structures in distinct solvent conditions, which can be a valuable guide for rigin analog design and rigidification of the bioactive conformation. In the present investigation, we extend our study and employ, in combination with high-temperature unrestrained MD simulations in *implicit* water ($\varepsilon = 80$), 1D and 2D ^{1}H NMR and CD spectroscopic techniques in aqueous PBS, pH 7.4, expecting that the exploration would presumably offer physiologically relevant bioactive conformation of rigin when bound to its receptor. We highlight the predominance of an unusual definable semi-folded *kinked* topology across the central Gln-Pro segment of rigin as a plausible molecular conformation that may be critical in orienting the functional side chains for recognition by the protein receptor.

Materials and Methods

Peptide Synthesis

The chemical synthesis of rigin was achieved using standard solution-phase procedures [21,22]. After catalytic hydrogenation (10% Pd-C in methanol), rigin was isolated and purified to homogeneity by MPLC system on a semi-preparative reversed-phase column (RP-18 LiChrosorb; Hibar Merck, 2.5 × 25 cm, 7-µm particles) using two separate isocratic solvent systems, i.e. 30 and 35% acetonitrile–water mixtures (v/v) containing 0.01% TFA. UV detection at 220 nm and a flow rate of 5 ml min^{-1} were used throughout purification. The purified rigin was obtained by lyophilizing fractions corresponding to the peak with $R_t = 20.8$ min. Both identity as well as purity of the synthetic rigin was ascertained by 300-MHz ^{1}H NMR spectra acquired in aqueous PBS, pH 7.4 (Supporting Information).

Energy Minimization and MD Simulations

In order to map the available conformational space of rigin, the zwitterionic structure with standard parameters for all-atom force field has been considered (Figure 1). Energy minimization and MD simulations were performed with TINKER version 4.2, using AMBER 99 force field [23]. A fully extended starting conformation ($\phi = \psi = \chi = \omega = 180^\circ$ and the ϕ_{Pro} was fixed to -65°) comprising L-residues was energy minimized to a 0.01 Å RMS gradient, using TNCG minimizer, available with TINKER molecular modeling suite of programs. The energy-minimized conformer with main-chain torsion angles, $\psi_{Gly} = 174.1^\circ$, $\phi_{Gln} = -152.6^\circ$, $\psi_{Gln} = 134.6^\circ$, $\phi_{Pro} = -73.2^\circ$, $\psi_{Pro} = -160.0^\circ$ and $\phi_{Arg} = -152.8^\circ$, was subjected to high-temperature MD simulations. To substantiate the experimental observations acquired in aqueous solution, MD simulation was performed under *implicit* water ($\varepsilon = 80$) at 900 K for 10 ns at constant number of particles, volume and temperature ensemble. The co-ordinates were saved every 4 ps to generate the trajectory of 2500 structures. Each structure was further energy minimized using TNCG method to a 0.01 Å RMS gradient and analyzed with the VMD [24] and MOLMOL [25] packages. All calculations and MD simulations were carried out on a Dell Precision Workstation 409 series.

NMR Spectroscopy

All 1D and 2D^{1}H NMR experiments were performed on a Bruker Avance DRX-300 FT-NMR instrument operating at an ambient temperature. A peptide concentration of ~3.0 mg in 0.5 ml of aqueous PBS, pH 7.4, was uniformly used for all the experiments. The water signal was partially suppressed using standard Bruker's WATERGATE [26] pulse program 'p3919gp' available with the instrument software library. The data acquisition parameters involved 128 scans with 4 dummy scans and an acquisition time of 4.5 s. The reported chemical shifts of the resonances

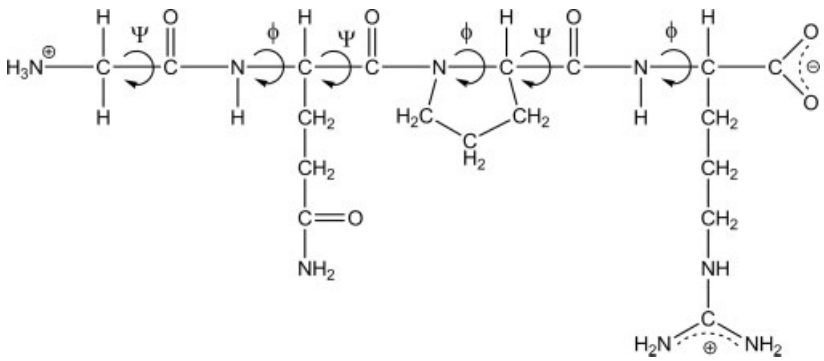

Figure 1. The zwitterionic chemical structure of rigin. The backbone torsion angles (ϕ and ψ) are indicated by arrows.

are with respect to the water signal observed at 4.80 ppm. The acquired data were processed at 16 K data points permitting direct measurement of the vicinal coupling constants $^3J_{N\alpha H}$. The ϕ torsion angles for the Gln and Arg residues were estimated within an uncertainty limit, via Karplus type relationship: $^3J_{N\alpha H} = A\cos^2\theta - B\cos\theta + C$ (where $\theta = |\phi - 60^\circ|$) [27,28]. The A, B and C constants recommended by Pardi *et al*. [29] were incorporated in the calculation. The complete resonance assignments were made on the basis of their characteristic spin systems and chemical shifts of the constituent residues from the combined use of 1D and 2D WATERGATE ^{1}H-^{1}H TOCSY and NOESY NMR experiments [27,28].

Phase-sensitive 2D TOCSY and NOESY experiments were carried out using time proportional phase increments, with the carrier on the water resonance for its presaturation. Water suppression parameters, the spin lock power setting and the mixing time delay of 200 ms, were used as justified and described previously [5,11]. The number of data points acquired along t_1 and t_2 were 256 $\times$ 1024, respectively. The 2D data were multiplied by a phase-shifted squared sine-bell apodization function and zero-filled twofold along both the dimensions, prior to Fourier transformation. The qualitative structural inferences deduced from the intensities of the NOE cross-peaks were categorized into three groups: strong ($d < 2.5$ Å), medium (2.5 Å $\leq d \leq$ 3.5 Å) and weak ($d \geq 4.5$ Å) [27,28]. Calibration of the spectrum was done with respect to the water resonance.

CD Spectroscopy

The CD spectra were recorded on a JASCO *J*810 spectropolarimeter at ambient temperature. The peptide solutions, at a concentration of 0.25 mg ml^{-1}, were prepared in aqueous PBS, pH 7.4, and milli-Q water, pH 4.8 and 8.5. A quartz cell with 0.1-cm path length was used. Both the optics and sample chamber were flushed with dry nitrogen gas throughout the experiments. Each spectrum is base line subtracted and representative of 16 consecutive scans acquired from 190 to 250 nm. Band intensities are expressed as molar ellipticities: $[\theta]_M$ degree cm^2 dmol^{-1}.

Results and Discussion

Energy Minimization and MD Simulations

To explore the accessible conformational space of rigin in polar aqueous environment, high-temperature unrestrained MD simulations were performed in *implicit* water. A significantly extended energy-minimized backbone structure, with all-*trans* peptide bonds ($\omega = \pm 179 \pm 1^\circ$), was subjected to MD simulations at 900 K for 10 ns (see the section on Materials and Methods). In view of experimental observation, the conformers with *cis* peptide bonds geometry (714 structures) across the Xaa-Pro peptide bond were eliminated from the analysis. Figure 2 shows the distribution of ϕ and ψ torsion angles of the Gln and Pro residues on the Ramachandran maps [30] for 1786 energy-minimized structures with all-*trans* peptide bonds. The conformers were analyzed in combination with various definable secondary structures, i.e. extended structures, a locally extended C_5-structure, inverse γ-turn structure and different β-turns from type I to type VIII β-turns, accessible to this short linear peptide [31–36]. Based on these definable secondary structural features, the resulting 292 structures could be grouped into five different families **A**– **E**.

Figure 3 shows the stereo views of the molecular structures of five superimposed families and Table 1 summarizes the averaged

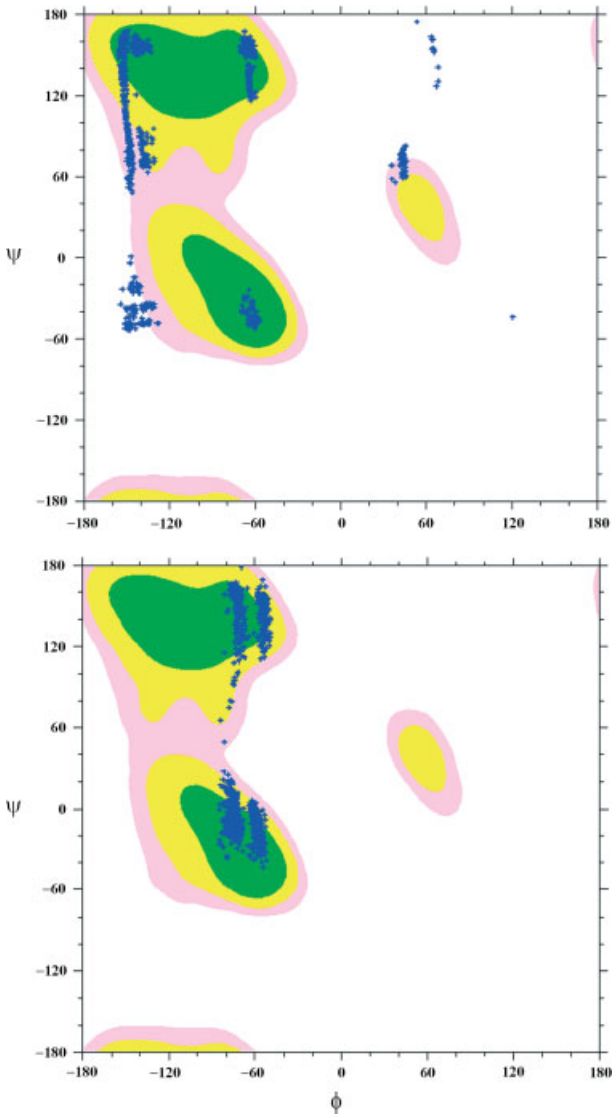

Figure 2. Ramachandran plots for the Gln (upper) and Pro (lower) residues of 1786 energy-minimized structures of rigin, with an all-*trans* peptide bond geometry.

ϕ and ψ torsion angles with their RMSD values. Regardless of two energetically preferred C$^\gamma$-*endo* and C$^\gamma$-*exo* orientations of the Pro residue, the backbone RMSD values of these families ranged between 0.30 and 0.49 Å. The five-membered pyrrolidine ring of the Pro residue invariably restricts the ϕ_{Pro} angles close to $-65 \pm 10^\circ$. One of the prominent features of the predicted conformations is the conservation of two central backbone torsion angles: $\psi_{Gln} \sim 155 \pm 10^\circ$ and $\phi_{Pro} \sim -65 \pm 10^\circ$, presented by the predominant families **A**–**D**. An examination of backbone torsion angles of various β-turn structures indicates that the set of torsion angles are adequate to define a type VII β-turn structure across the central Gln-Pro segment. While analyzing the presence of chain reversal in globular proteins, Lewis *et al*. (1973) originally defined the type VII β-turn structure as a *kink* in the polypeptide chain and a combination of backbone torsion angles: $|\psi_{i+1}| \geq 140^\circ$ and $|\phi_{i+2}| \leq 60^\circ$ or $|\psi_{i+1}| \leq 60^\circ$ and $|\phi_{i+2}| \geq 140^\circ$ characterized its existence [31]. In all the five families, the ψ torsion angles of the *N*-terminus achiral Gly residue are close to a semi-extended conformation ($\psi_{Gly} \sim \pm 100 \pm 10^\circ$), i.e. $\psi_{Gly} \sim 100^\circ$

Journal of PeptideScience

Table 1. The averaged main-chain (ϕ and ψ) and side-chain (χ) torsion angles (°) of the five MD-simulated families **A**–**E**, with their standard deviations (Å), of rigin in *implicit* water

Families	A	B	C	D	E
No. of structures	92	94	63	31	12
RMSD[a]	0.39	0.38	0.38	0.41	0.49
RMSD[b]	1.81	1.86	1.76	1.76	1.64
Gly					
ψ_1	100.7 ± 8.9	−97.4 ± 1.3	−101.2 ± 1.0	−109.5 ± 21.2	−103.3 ± 11.2
Gln					
ϕ_2	−143.0 ± 2.9	−66.9 ± 0.7	−142.9 ± 2.5	−141.9 ± 3.8	−65.2 ± 3.2
ψ_2	155.7 ± 2.2	154.7 ± 2.8	155.7 ± 2.6	154.7 ± 2.8	−39.7 ± 5.6
χ_1	−70.1 ± 3.3	−68.1 ± 2.9	−69.8 ± 2.9	−69.1 ± 3.1	−64.7 ± 4.3
Pro					
ϕ_3	−66.2 ± 9.0	−68.3 ± 8.4	−67.9 ± 8.7	−56.2 ± 1.2	−67.9 ± 9.1
ψ_3	−11.7 ± 9.4	−7.7 ± 8.8	−9.5 ± 9.2	−154.5 ± 7.5	−15.7 ± 13.2
Arg					
ϕ_4	−147.8 ± 5.1	−147.1 ± 4.6	−147.6 ± 4.9	−144.6 ± 10.6	−146.3 ± 9.2

[a] RMSD without Gln and Arg side chains.
[b] RMSD with Gln and Arg side chains.

in families **A** and ∼ −100 ± 10° in families **B**–**E**, whereas the ϕ torsion angles of the *C*-terminal Arg residue are essentially restricted to an extended conformation, i.e. ϕ_{Arg} ∼ −145 ± 10°. However, the ψ_{Pro} angles prefer two distinct conformations, i.e. the folded ψ_{Pro} ∼ −10 ± 10° in families **A**–**C** and **E**, and significantly extended ψ_{Pro} ∼ 155 ± 10° in family **D**. A careful analysis of the MD-simulated families suggests that in *implicit* water, the preferred unusual conformations of rigin may be presented as a *kinked* topology, classified as type VII β-turn, across the central Gln-Pro segment and the *N*- and *C*-terminal residues prefer semi-extended and extended conformations, respectively.

1D and 2D ^{1}H NMR Spectroscopic Studies

The experimental supports for the existence of an unusual solution conformation of rigin in aqueous environments were obtained from 1D and 2D ^{1}H NMR spectroscopic studies. Figure 4 shows a partially well-resolved, fully assigned 1D ^{1}H NMR spectrum (∼ 6.0 to 9.0 ppm) of rigin in aqueous PBS, pH 7.4, and the observed chemical shifts and $^3J_{N\alpha H}$ coupling constants of the Gln and Arg residues are summarized in Table 2. An observation of two sets of resonances in the 1D ^{1}H NMR spectrum at room temperature has been attributed to *cis*–*trans* isomerization across the Xaa-Pro peptide bond. The existence of major *trans* conformer (∼ 88%) as predominant population was confirmed from the observation of an intense interresidue Gln $C^\alpha H$ ↔ Pro $C^\delta H_2$ NOE cross-peaks, i.e. $d_{\alpha\delta(i,\,i+1)}$ NOE [27,28]. In the present study, we therefore investigated the conformational characteristics of rigin with all-*trans* peptide bonds. The absence of broadening of the ^{1}H NMR resonances supports the notion that the peptide is monomeric under the experimental condition.

The preliminary information regarding the existence of ordered folded conformations of rigin in aqueous PBS was obtained from the characteristic conformational chemical shifts of the $C^\alpha H$ resonances of the constituent residues [37–39]. The $C^\alpha H$ chemical shift deviation from unstructured values ($_\Delta\delta_{H\alpha} = \delta^{obs}_{H\alpha} - \delta^{rc}_{H\alpha}$; where $\delta^{obs}_{H\alpha}$ and $\delta^{rc}_{H\alpha}$ are the observed and random-coil chemical shifts, respectively) is diagnostic of ordered backbone conformations. In general, negative $\Delta\delta_{H\alpha}$ values are for helical or folded β-turn structures and positive for extended conformations. The positive $\Delta\delta_{H\alpha}$ value of ∼ 0.36 ppm for the Gln residue is clearly indicative of significantly extended backbone conformations, which also correlates with the observed $^3J_{NH\alpha}$ value in view of coherence of chemical shifts of the $C^\alpha H$ resonances. The slight upfield $C^\alpha H$ chemical shifts of ∼ 0.02 ppm for the Pro residue may signify that the ψ_{Pro} angle is unlikely to be restricted to an extended conformation.

Table 2. The observed ^{1}H NMR chemical shifts (ppm) and $^3J_{NH\alpha}$ coupling constants (Hz) of rigin in aqueous PBS, pH 7.4, at an ambient temperature

Residues	NH	$C^\alpha H$	$C^\beta H$	Others	$^3J_{HNC^\alpha H}$
Gly	NO[a]	3.87	–	–	–
Gln	8.66	4.18[b]	$C^\beta H'$ – 2.13 $C^\beta H''$ – 2.07	$C^\gamma H_2$ – 2.43 $N^\delta H$ (S1) – 7.63 $N^\delta H$ (S2) – 6.92	6.0
Pro	–	4.40	$C^\beta H_2$ – 2.13	$C^\gamma H_2$ – 2.00 $C^\delta H'$ – 3.82 $C^\delta H''$ – 3.70	–
Arg	8.14	4.14	$C^\beta H_2$ – 1.95	$C^\gamma H_2$ – 1.65 $C^\delta H_2$ – 3.22 $N^\varepsilon H$ – 7.24 $N^\eta H$ – 6.81	6.9

[a] Not observed.
[b] Overlapping with H_2O peak.

The observed $^3J_{N\alpha H}$ value of 6.0 Hz for the Gln NH suggests that the ϕ angle may be restricted to approximately 35°, 85°, −75° or −160°. The results of MD simulations clearly disallow the positive ϕ_{Gln} value and therefore the solution conformation is expected to accommodate ϕ_{Gln} ∼ −75° or −160°. The later extended ϕ_{Gln} value sustains and reinforces the conformations offered by the three predominant families **A, C** and **D**. Likewise, the $^3J_{N\alpha H}$ value of 6.9 Hz for the Arg residue may suggest that the ϕ_{Arg} is likely to be restricted to approximately either −90° or −150°. The extended ϕ_{Arg} value is evidently in conformity with the

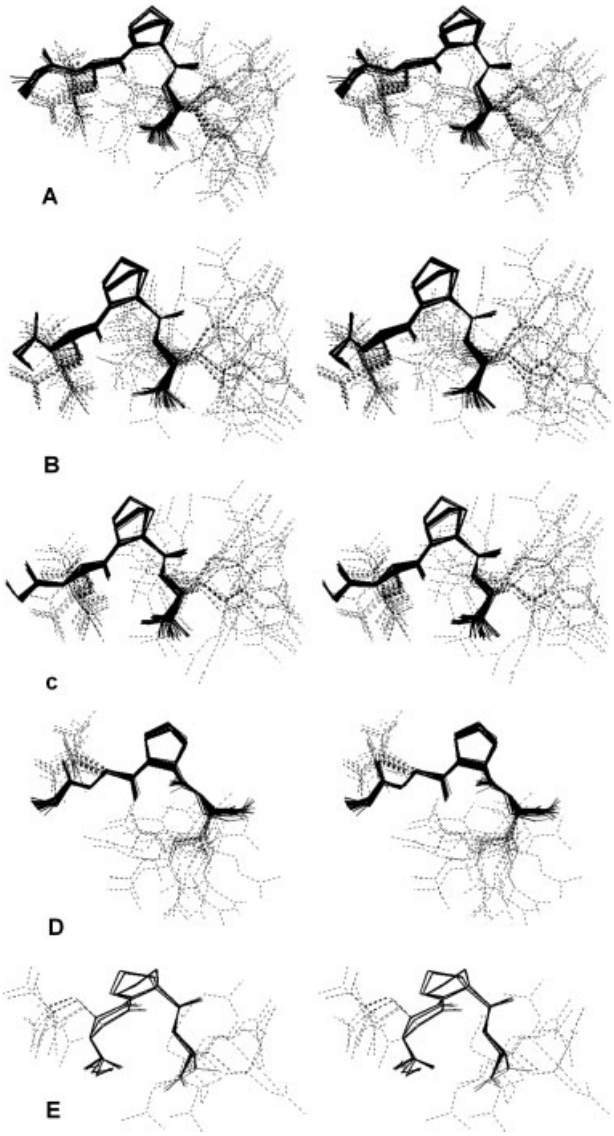

Figure 3. Stereo views of superimposed molecular structures of five MD-simulated families: family **A** (92 structures), family **B** (94 structures), family **C** (63 structures), family **D** (22 structures) and family **E** (12 structures) of rigin in *implicit* water. The dynamic fluctuations of the Gln and Arg side chains are presented by dotted lines.

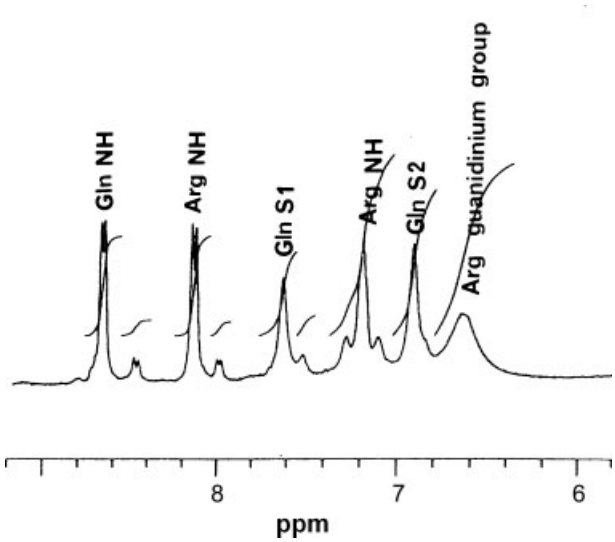

Figure 4. Partial 1D ^{1}H NMR spectrum of rigin (6.0–9.0 ppm) in PBS, pH 7.4. Resonance assignments of the predominant conformer with an all-*trans* peptide bonds are indicated.

MD-simulated structures offered by all the five families. Therefore, the experimentally deduced ϕ values for the Gln and Arg residues incline us to propose that the preferred molecular conformations of rigin in aqueous PBS may be presented by families **A, C** and **D**. However, it may be emphasized that 'as a general rule of thumb, helices exhibit $^{3}J_{NH\alpha} < 6$ Hz, β-sheets exhibit $^{3}J_{NH\alpha} > 8$ Hz, and random extended chains exhibit $^{3}J_{NH\alpha} = 6-8$ Hz. Note, however, that deviations from this rule occur when proline is present' [28].

Strong evidence for the predominance of a definable type VII β-turn structure across the central Gln-Pro segment of rigin is provided by the observed NOE cross-peaks in a 2D NOESY spectrum. Figure 5 shows the NOESY spectrum highlighting critical inter- and intraresidue NOEs acquired in aqueous PBS. The short linear peptides in solution typically represent an ensemble of flexible structures [27,28,40,41] and therefore observations of a number of strong inter- and intraresidue NOEs at an ambient temperature all pointing toward significant conformational inflexibility in solution. The conformation largely consistent with molecular modeling and various ^{1}H NMR-derived parameters is shown in Figure 6. The presence of a strong Gly $C^{\alpha}H_2 \leftrightarrow$ Gln NH interresidue NOE connectivity, i.e. $d_{\alpha N(i,\, i+1)}$ NOE, clearly suggests that the ψ torsion angle of the achiral Gly residue may be restricted to a significantly extended conformation, i.e. $\psi_{Gly} \sim \pm 100 \pm^{\circ}$. Simultaneous observation of a strong Gln $C^{\alpha}H \leftrightarrow$ Pro $C^{\delta}H'$ and a medium Gln $C^{\alpha}H \leftrightarrow$ Pro $C^{\delta}H''$ interresidue NOE, besides confirming the presence of the *trans* Gln-Pro imide bond, also indicates that the ψ_{Gln} adopts an extended conformation, i.e. $\psi_{Gln} \sim 145 \pm 10^{\circ}$, a value essentially consistent with MD-simulated families **A, C** and **D**. The ψ_{Gln} close to $\pm 60^{\circ}$ is most likely to be energetically disfavored due to non-bonded interactions. This conclusion is primarily borne out by the extensive conformational energy calculations performed by Zimmerman and Scheraga [42] on Ac-Xaa-Pro-NHMe model system (where, Xaa = Ala, Asn, Gly or Pro) using an Emperical Conformational Energy Program for Peptides. The analysis revealed that the Pro residue severely limits the conformational space of the preceding residue but not of the one which follows it and therefore conformations of Xaa-Pro with $|\psi_{i+1}| \leq 70^{\circ}$ are usually disallowed due to unfavorable interaction between the Pro C^{δ} atom and the backbone amide-NH or $C^{\beta}H_2$ group of the preceding residue [42,43].

An observation of a fairly strong Pro $C^{\alpha}H \leftrightarrow$ Arg NH NOE may suggest that the ψ torsion angle of the Pro residue prefers an extended conformation, provided the ϕ_{Arg} is restricted close to -145°. In fact, a medium range $d_{\alpha N(i,\, i+1)}$ NOE is expected for the folded ψ value. It must be noted that during MD simulations, the ψ_{Pro} torsion angle is largely restricted to two distinct energetically favorable conformations: $\psi_{Pro} \sim 0^{\circ}$ (folded or *bridge* region) and $\psi_{Pro} \sim 145^{\circ}$ (extended or polyproline II region), and as evident from Figure 7, the former ψ_{Pro} value is prevalent, i.e. ~70%. Therefore, it is reasonable to presume that the ψ_{Pro} angle of rigin in an aqueous environment might not be entirely restricted to polyproline II region and a dynamic equilibrium involving the ψ_{Pro} angle could prevail between folded and extended conformers while retaining the characteristic *kink* of a type VII β-turn structure.

Journal of PeptideScience

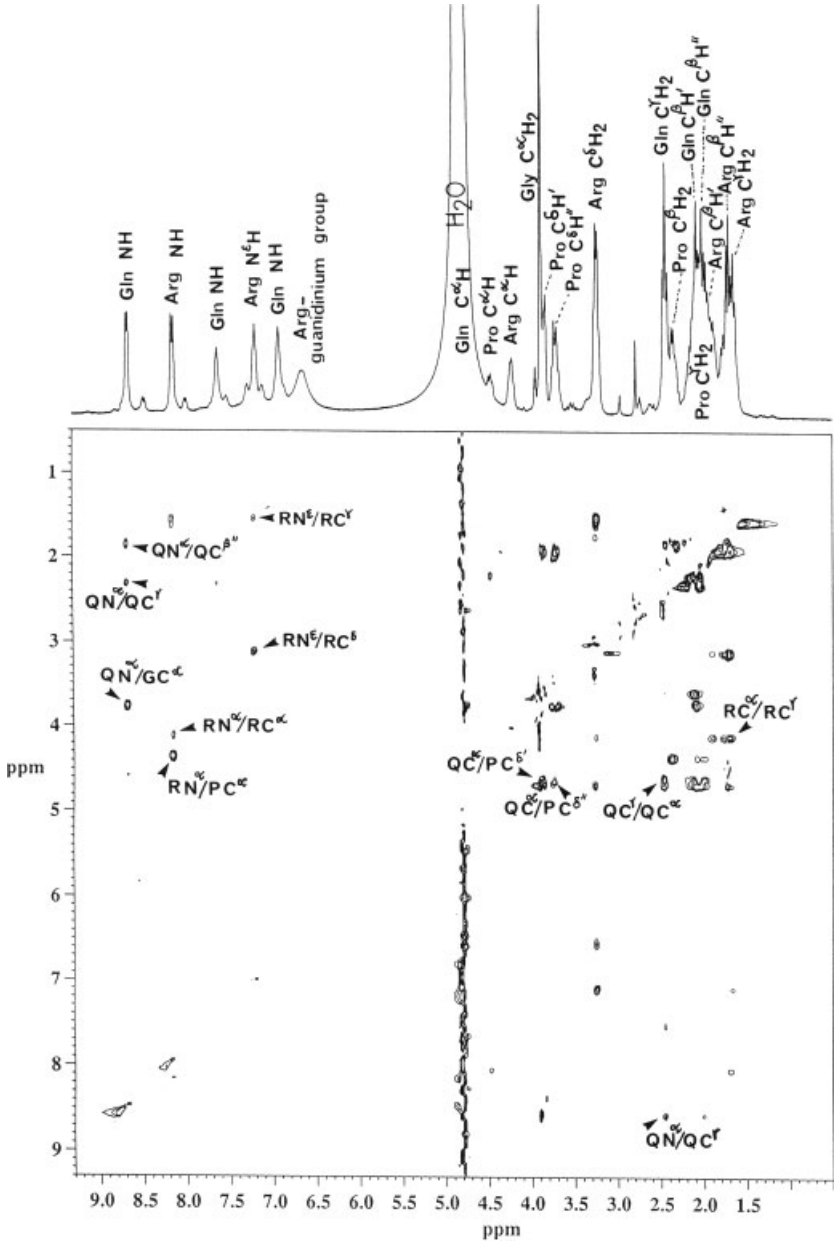

Figure 5. The observed 300-MHz 2D ^{1}H-^{1}H NOESY spectrum of rigin in PBS, pH 7.4. The critical NOE cross-peaks suited for structural interpretation are indicated by arrows.

Although the high-temperature MD simulations of rigin in *implicit* water revealed significant dynamic fluctuations of the Gln and Arg side chains, the experimental 1D and 2D ^{1}H NMR-derived parameters rather suggest pre-organization of functional side chains in aqueous PBS. The observation of a few main-chain to side-chain intraresidue NOEs provides evidence regarding their restricted non-random orientations. For instance, for the restricted $\phi_{\mathrm{Gln}} \sim -145^{\circ}$, the simultaneous observation of the two medium intense Gln $C^{\beta}H''$ $\leftrightarrow$ Gln NH $\leftrightarrow$ Gln $C^{\gamma}H_2$ NOEs indicates that the χ_1 torsion angle assumes a folded *gauche* orientation [27,28]. Likewise, the co-existence of a medium Arg NH $\leftrightarrow$ Arg $C^{\beta}H''/C^{\gamma}H_2$ and a weak Arg NH $\leftrightarrow$ Arg $C^{\alpha}H$ intense NOEs allow us to infer that the Arg χ_1 also prefers a *gauche* orientation, albeit with some deviation, provided the ϕ_{Arg} angle is restricted to approximately -145°. Also, the simultaneous occurrence of a strong and a weak Arg $C^{\alpha}H_2 \leftrightarrow$ Arg $C^{\gamma}H_2 \leftrightarrow$ Arg $N^{\varepsilon}H$ NOEs may signify limited motion of the Arg side chain involving the $\chi_1 - \chi_3$ torsion angles.

The results of MD simulations performed in *implicit* water indicate that rigin is capable of assuming a number of low-energy conformers. Nevertheless, an accommodation of type VII β-turn structure across Gln-Pro segment appears to prevail, because a number of experimentally derived 1D and 2D ^{1}H NMR parameters substantiate the prevalence of this element of secondary structure. In conjunction with conformational $\Delta\delta_{\mathrm{H}\alpha}$ values, $^{3}J_{\mathrm{N}\alpha\mathrm{H}}$ coupling constants of the Gln and Arg residues and the magnitudes of experimentally observed NOEs, it is reasonable to propose that closely related structures offered by families **A, C** and **D** might be in dynamic equilibrium and subtle conformational deviations may transpire at the central part of the molecule involving the ψ_{Pro} angle. The preferred torsion angles: $\psi_{\mathrm{Gly}} \sim \pm 100^{\circ}$,

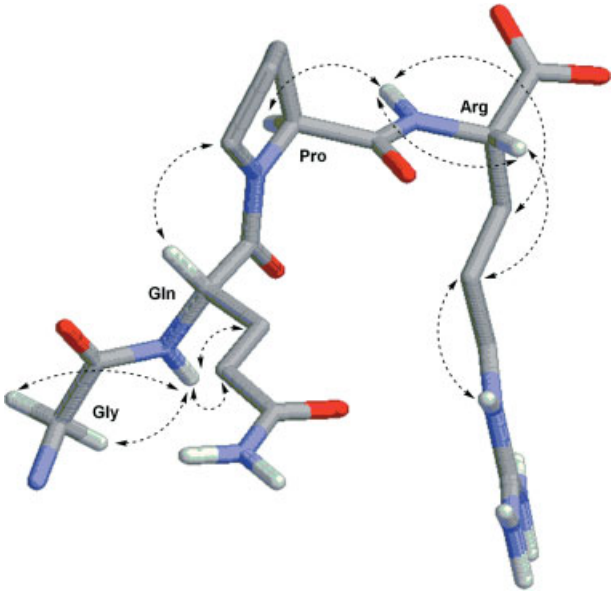

Figure 6. The proposed solution conformation of rigin in aqueous PBS as derived from molecular modeling and ^{1}H NMR-derived parameters. The dotted lines with double-edged arrows highlight the observed inter- and intraresidue NOE cross-peaks.

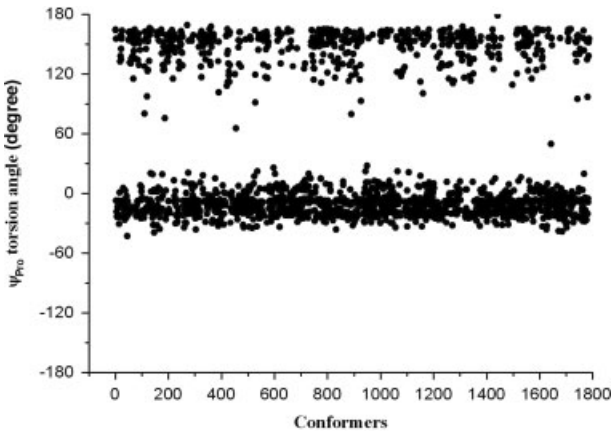

Figure 7. The two distinct populations of ψ_{Pro} torsion angles for 1786 conformers of rigin with an all-*trans* peptide bonds, i.e. folded ψ_{Pro} in the *bridge* region (~70%) and significantly extended ψ_{Pro} in the polyproline II region (~30%), observed during the MD simulations.

$\phi_{Gln} \sim -145^\circ$, $\psi_{Gln} \sim 155^\circ$, $\phi_{Pro} \sim -65^\circ$, $\psi_{Pro} \sim -10^\circ$ or 155°, $\phi_{Arg} \sim -145^\circ$ may characterize the semi-folded *kinked* topology which lie within the energetically allowed conformational space of the Ramachandran map. A notable outcome of our MD simulation study is the observation of appreciably increased Gly $C^\alpha \cdots C^\alpha$ Arg distance, i.e. $d(C^\alpha_i \cdots C^\alpha_{i+3}) \geq 8.2$ Å in families **A**–**D** and significantly reduced $d(C^\alpha_i \cdots C^\alpha_{i+3}) \sim 5.3$ Å in the minor family **E**. The conformation presented by family **E** (12 structures) exhibits a close resemblance with a folded type I (or III) β-turn; however, this receives almost no support from the experimental ^{1}H NMR-derived parameters.

CD Spectroscopic Studies

To further enumerate the structural characteristics of rigin, CD experiments [44,45] were performed in aqueous as well as in non-aqueous structure-promoting solvents, 197 i.e. apolar, hydrophobic TFE and polar, hydrogen bond-accepting TMP. As evident from Figure 8, the CD characteristics of rigin are strongly solvent dependent. The observed CD spectrum of rigin in aqueous PBS, pH 7.4, is characterized by an intense negative band at ~198 nm ($[\theta]_M \sim -42\,700$) and an extremely weak negative shoulder at ~ 234 nm ($[\theta]_M \sim -1500$). The CD spectral patterns remain almost unaltered in water at pH 4.8 and pH 8.5, i.e. characterized by an intense negative band at ~ 197 nm ($[\theta]_M \sim -41\,900 \pm 300$) and a weak negative shoulder at ~ 234 nm ($[\theta]_M \sim -800 \pm 50$), indicative of substantial conformational similarities. The appearance of a weak shoulder at ~ 234 nm may suggest a small proportion of non-random ordered structures in aqueous solution. Interestingly, in TFE, the CD spectrum showed a prominent negative maximum at ~ 221 nm ($[\theta]_M \sim -12\,110$) and positive ellipticity centered at ~ 194 nm ($[\theta]_M \sim 6910$). On the other hand, in TMP, the CD curve is characterized by a broad positive doublet centered at ~ 216 nm ($[\theta]_M \sim 9420$) and ~ 209 nm ($[\theta]_M \sim 8780$), well above ~ 200 ± 3 nm. The overall CD results indicate the ability of rigin sequence to undergo large conformational changes under the influence of solvent polarities. However, it must be reiterated that it is not easy to distinguish and assign specific conformational ensembles of folded or semi-folded β-turn variants on the basis of CD spectra alone [11,32,45] and the structural insight must be provided by supplementing the data via theoretical and/or experimental 1D and 2D ^{1}H NMR analysis, as discussed above.

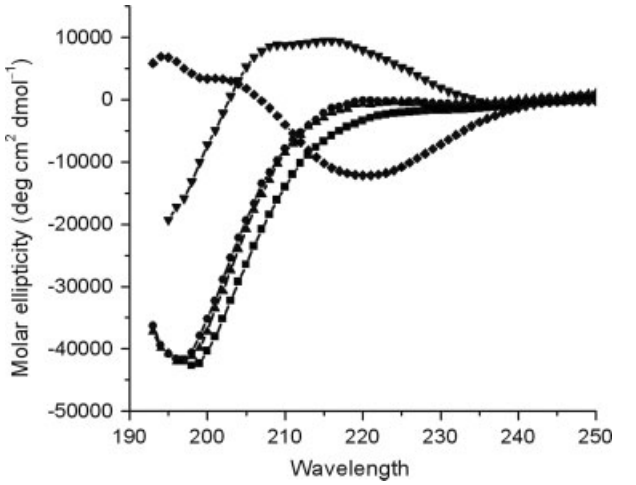

Figure 8. A comparison of CD spectra of rigin in aqueous and non-aqueous environments: PBS pH 7.4 (■—■), water pH 4.8 (●—●), water pH 8.5 (▲—▲), TFE (♦—♦) and TMP (▼—▼).

Although the two immunomodulators, rigin and tuftsin, apparently exhibit remarkably similar phagocytosis-stimulating activities, their conformational properties appear to be quite different. Our contention is purely based on extensive theoretical as well as experimental conformational analysis reported for the two immunomodulators in aqueous as well as non-aqueous polar environments [1–12]. The available literature suggests that the β-turn and/or *inverse* γ-turn structures stabilized by a strong intramolecular hydrogen bond can be accessed by the tuftsin molecule, whereas our systematic conformational explorations signify the subsistence of an unfolded, non-γ-turn structure for rigin. We advocate that a type VII β-turn like topology, not stabilized by any intramolecular interaction, constitutes the scaffold upon which energetically preferred functional side

Journal of PeptideScience

chains pre-organize, for recognition and binding to target protein receptor. A careful analysis of polypeptide chain reversals in globular proteins revealed that the majority of type VII β-turns, seven out of eight, are actually devoid of the typical 4 $\rightarrow$ 1 intramolecular hydrogen bond [46,47].

Conclusions

Our systematic conformational analysis of an immunomodulator rigin in *implicit* water established the accommodation of an unusual type VII β-turn structure or *kinked* topology across the central Gln-Pro segment. Sampling with *implicit* solvent yielded remarkable similarities between the preferred predominant conformers and the conformations derived from a variety of 1D and 2D ^{1}H NMR parameters acquired in aqueous PBS solution. A combination of theoretical MD simulations and experimental ^{1}H NMR and CD spectroscopic studies lead to the most detailed insight of a semi-folded *kinked* topology not stabilized by intramolecular interaction. Neither MD simulations nor ^{1}H NMR data alone suffice to address the issue of conformational ensembles of this rare secondary structure. The analysis undoubtedly signifies that occasionally the primary structure may be adequate to give rise to required conformational propensities of small peptides and such unusual secondary structural features may be considered biologically relevant. Whether the two energetically accessible and distinct conformations of rigin, i.e. a type VII β-turn scaffold and a *distorted* type III (or I) β-turn motif, are effectively recognized by the rigin receptor remains to be established. Nevertheless, in the absence of any X-ray crystallographic analysis, the available conformational models may provide means of initiating the design of rigin analogs and derivatives capable of exhibiting significant immunostimulating activity (unpublished results).

Acknowledgements

The work was supported by the Council of Scientific & Industrial Research, Government of India. We are grateful to Drs CM Gupta and R Roy for facilitating the NMR work at CDRI, Lucknow. RK thanks Dr P Guptasarma for critically reading the manuscript. NK wishes to acknowledge CSIR for the fellowship. This is IMTech Communication No. 042/09.

Supporting information

Supporting information may be found in the online version of this article.

References

1 Veretennikova NI, Chipens GI, Nikiforovich GV, Betinsh YR. Rigin: another phagocytosis-stimulating tetrapeptide isolated from human IgG. Confirmations of a hypothesis. *Int. J. Pept. Protein Res.* 1981; **17**: 430–435.
2 Rocchi R, Biondi L, Cavaggion F, Filira F, Gobbo M, Dagan S, Fridkin M. Synthesis and biological activity of tuftsin and rigin derivatives containing monosaccharides or monosaccharide derivatives. *Int. J. Pept. Protein Res.* 1987; **29**: 262–275.
3 Siemion IZ, Kluczyk A. Tuftsin: on the 30-year anniversary of Victor Najjar's discovery. *Peptides* 1999; **20**: 645–674.
4. Dutta RC, Puri A, Anand N. Immunomodulatory potential of hydrophobic analogs of rigin and their role in providing protection against *Plasmodium berghei* infection in mice. *Int. Immunopharmacol.* 2001; **1**: 843–855.
5 D'Ursi A, Pegna M, Amodeo P, Molinari H, Verdini A, Zetta L, Temussi PA. Solution conformation of tuftsin. *Biochemistry* 1992; **31**: 9581–9586.
6 O'Connor SD, Smith PE, al-Obeidi F, Pettitt BM. Quenched molecular dynamics simulations of tuftsin and proposed cyclic analogues. *J. Med. Chem.* 1992; **35**: 2870–2881.
7 Werner GH, Jollés P. Immunostimulating agents: what next? A review of their present and potential medical applications. *Eur. J. Biochem.* 1996; **242**: 1–19.
8 Gershonov E, Granoth R, Tzehoval E, Gaoni Y, Fridkin M. 1-Aminocyclobutane-carboxylic acid derivatives as novel structural elements in bioactive peptides: application to tuftsin analogs. *J. Med. Chem.* 1996; **39**: 4833–4843.
9 Fridkin M, Tsubery H, Tzehoval E, Vonsover A, Biondi L, Filira F, Rocchi R. Tuftsin-AZT conjugate: potential macrophage targeting for AIDS therapy. *Pept. Sci.* 2005; **11**: 37–44.
10 Ashish, Kishore R. Further support for the conformational preferences for a type VII β-turn structure in bioactive tetrapeptides: tuftsin and rigin. In *Peptides Biology and Chemistry: Proceedings of the 2000 Chinese Peptide Symposium*, Xu J-C, Xu H-Y, Tam JP (eds). Science Press: Beijing, China, 2002; 139–146.
11 Ashish, Grover A, Kishore R. Characterization of a novel type VII β-turn conformation for a bio-active tetrapeptide rigin A synergy between theoretical and experimental results. *Eur. J. Biochem.* 2000; **267**: 1455–1463.
12 Ashish, Kishore R. Folded conformation of an immunostimulating tetrapeptide rigin: high temperature molecular dynamics simulation study. *Bioorg. Med. Chem.* 2002; **10**: 4083–4090.
13 Bump NJ, Lee J, Wleklik M, Reichler J, Najjar VA. Isolation and subunit composition of tuftsin receptor. *Proc. Nat. Acad. Sci. U.S.A.* 1986; **83**: 7187–7191.
14 von Wronski MA, Raju N, Pillai R, Bogdan NJ, Marinelli ER, Nanjappan P, Ramalingam K, Arunachalam T, Eaton S, Linder KE, Yan F, Pochon S, Tweedle MF, Nunn AD. Tuftsin binds neuropilin-1 through a sequence similar to that encoded by exon 8 of vascular endothelial growth factor. *J. Biol. Chem.* 2006; **281**: 5702–5710.
15 Adcock SA, McCammon JA. Molecular dynamics: survey of methods for simulating the activity of proteins. *Chem. Rev.* 2006; **106**: 1589–1615.
16 Muñoz V. Conformational dynamics and ensembles in protein folding. *Annu. Rev. Biophys. Biomol. Struct.* 2007; **36**: 394–412.
17 Chen J, Brooks CL, Khandongin J. Recent advances in implicit solvent based methods for biomolecular simulations. *Curr. Opin. Struct. Biol.* 2008; **18**: 140–148.
18 Nikiforovich GV. Computational molecular modeling in peptide drug design. *Int. J. Pept. Protein Res.* 1994; **44**: 513–531.
19 Wonopil IM, Jianhan C, Brooks CL III. Peptide and proteins folding and conformational equilibria: theoretical treatment of electrostatic and hydrogen bonding with implicit solvent model. *Adv. Protein Chem.* 2005; **72**: 173–198.
20 van der Kamp MW, Shaw KE, Woods CJ, Mulholland AJ. Biomolecular simulation and modelling: status, progress and prospects. *J. R. Soc. Interface* 2008; **5**: S173–S190.
21 Bodansky M, Bodansky A. *The Practice of Peptide Synthesis*, 2nd edn. Springer-Verlag: New York, 1994.
22. Okada Y. Synthesis of peptides by solution methods. *Curr. Org. Chem.* 2001; **5**: 1–43.
23 Ponder JW. *TINKER: software tools for molecular design*, 4.2 edn, Washington University School of Medicine: Saint Louis, MO, 2004.
24 Humphrey W, Dalke A, Schulten K. VMD-visual molecular dynamics. *J. Mol. Graph.* 1996; **14**: 33–38.
25 Koradi R, Billeter M, Wüthrich K. MOLMOL: a program for display and analysis of macromolecular structures. *J. Mol. Graph.* 1996; **14**: 51–55.
26 Piotto M, Saudek V, Sklenar V. Gradient-tailored excitation for single-quantum NMR spectroscopy of aqueous solutions. *J. Biomol. NMR* 1992; **2**: 661–665.
27 Wüthrich K. *NMR of Proteins and Nucleic Acids*. John Wiley & Sons: New York, 1986.
28 Evans JNS. *Biomolecular NMR Spectroscopoy*. Oxford University Press: Oxford, 1995.
29 Pardi A, Billeter M, Wüthrich K. Calibration of the angular dependence of the amide proton-C$^\alpha$ proton coupling constants, $^3J_{HN\alpha}$, in a globular protein. Use of $^3J_{HN\alpha}$ for identification of helical secondary structure. *J. Mol. Biol.* 1984; **180**: 741–751.

30 Ramachandran GN, Sasisekharan V. Conformation of polypeptides and proteins. *Adv. Protein Chem.* 1968; **23**: 283–438.
31 Lewis PN, Momany FA, Scheraga HA. Chain reversals in proteins. *Biochim. Biophys. Acta.* 1973; **303**: 211–229.
32 Rose GD, Gierasch LM, Smith JA. Turns in peptides and proteins. *Adv. Protein. Chem.* 1985; **37**: 1–109.
33 Wilmot CM, Thornton JM. Analysis and prediction of the different types of beta-turn in proteins. *J. Mol. Biol.* 1988; **203**: 221–232.
34 Richardson JS, Richardson DC. Principles and patterns of protein conformation. In *Prediction of Protein Structure and the Principles of Protein Conformation*, Fasman GD (ed.). Plenum Press: New York and London: 1990; 1–98.
35 Thakur AK, Ashish, Kishore R. Novel hydrogen bonding ring motifs in a model peptide: crystal and molecular conformation. *Chem. Commun.* 1999; 1643–1644.
36 Venkatraman J, Shankaramma SC, Balaram P. Design of folded peptides. *Chem. Rev.* 2001; **101**: 3131–3152.
37 Wishart DS, Sykes BD. Chemical shifts as a tool for structure determination. *Methods Enzymol.* 1994; **239**: 363–392.
38 Merutka G, Dyson HJ, Wright PE. Random coil ^{1}H chemical shifts obtained as a function of temperature and trifluoroethanol concentration for the peptide series GGXGG. *J. Biomol. NMR* 1995; **5**: 14–24.
39 Wishart DS, Case DA. Use of chemical shifts in macromolecular structure determination. *Methods Enzymol.* 2001; **338**: 3–34.
40 Dyson HJ, Wright PE. Defining solution conformations of small linear peptides. *Annu. Rev. Biophys. Biophys. Chem.* 1991; **20**: 519–538.
41 Serrano L. The relationship between sequence and structure in elementary folding units. *Adv. Protein Chem.* 2000; **53**: 49–85.
42 Zimmerman SS, Scheraga HA. Influence of local interactions on protein structure. I. Conformational energy studies of N-acetyl-*N*′-methylamides of Pro-X and X-Pro dipeptides. *Biopolymers* 1977; **16**: 811–843.
43 Prasad BVV, Balaram P. The stereochemistry of peptides containing α-aminoisobutyric acid. *CRC Crit. Rev. Biochem.* 1984; **16**: 307–348.
44 Goodman M, Verdini AS, Toniolo C, Phillips WD, Bovey FA. Sensitive criteria for the critical size for helix formation in oligopeptides. *Proc. Nat. Acad. Sci. U.S.A.* 1969; **64**: 444–450.
45 Fasman GD. *Circular Dichroism and the Conformational Analysis of Biolmolecules*. Plenum Press: New York and London, 1996.
46 Chou PY, Fasman GD. Beta-turns in proteins. *J. Mol. Biol.* 1977; **115**: 135–175.
47 Richardson JS. The anatomy and taxonomy of protein structure. *Adv. Protein Chem.* 1981; **34**: 167–339.

